Biochimica et Biophysica Acta 1838 (2014) 756–765

Contents lists available at ScienceDirect

Biochimica et Biophysica Acta

journal homepage: www.elsevier.com/locate/bbamem

Differential functional rescue of Lys^{513} and Lys^{516} processing mutants of MRP1 (ABCC1) by chemical chaperones reveals different domain–domain interactions of the transporter

Surtaj H. Iram [1], Susan P.C. Cole *

Division of Cancer Biology and Genetics, Queen's University, Kingston, ON K7L 3N6, Canada
Department of Pathology & Molecular Medicine, Queen's University, Kingston, ON K7L 3N6, Canada

ARTICLE INFO

Article history:
Received 10 September 2013
Received in revised form 24 October 2013
Accepted 4 November 2013
Available online 11 November 2013

Keywords:
ATP-binding cassette
Multidrug resistance protein 1
Organic anion transporter
Plasma membrane trafficking
Protein misfolding
Chemical chaperones

ABSTRACT

Multidrug resistance protein 1 (MRP1) extrudes drugs as well as pharmacologically and physiologically important organic anions across the plasma membrane in an ATP-dependent manner. We previously showed that Ala substitutions of Lys^{513} and Lys^{516} in the cytoplasmic loop (CL5) connecting transmembrane helix 9 (TM9) to TM10 cause misfolding of MRP1, abrogating its expression at the plasma membrane in transfected human embryonic kidney (HEK) cells. Exposure of HEK cells to the chemical chaperones glycerol, DMSO, polyethylene glycol (PEG) and 4-aminobutyric acid (4-PBA) improved levels of K513A to wild-type MRP1 levels but transport activity was only fully restored by 4-PBA or DMSO treatments. Tryptic fragmentation patterns and conformation-dependent antibody immunoreactivity of the transport-deficient PEG- and glycerol-rescued K513A proteins indicated that the second nucleotide binding domain (NBD2) had adopted a more open conformation than in wild-type MRP1. This structural change was accompanied by differences in ATP binding and hydrolysis but no changes in substrate K_m. In contrast to K513A, K516A levels in HEK cells were not significantly enhanced by chemical chaperones. In more permissive insect cells, however, K516A levels were comparable to wild-type MRP1. Nevertheless, organic anion transport by K516A in insect cell membranes was reduced by >80% due to reduced substrate K_m. Tryptic fragmentation patterns indicated a more open conformation of the third membrane spanning domain of MRP1. Thus, despite their close proximity to one another in CL5, Lys^{513} and Lys^{516} participate in different interdomain interactions crucial for the proper folding and assembly of MRP1.

1. Introduction

Multidrug resistance protein 1 (MRP1) is an ATP-binding cassette (ABC) transporter that mediates the ATP-dependent efflux of a wide variety of structurally diverse compounds across the plasma membrane. Among the nine drug transporters within the 'C' sub-family of the ABC superfamily, MRP1 (ABCC1) is the most commonly associated with clinical multidrug resistance, a major cause of failure of chemotherapy in cancer patients. In addition to anticancer agents, MRP1 mediates the ATP-dependent efflux of a variety of organic anions that include both endogenous metabolites and exogenous xenobiotics, many of which are conjugated to glutathione (e.g. the cysteinyl leukotriene C_4 (LTC_4)) or glucuronide (e.g. estradiol glucuronide, ($E_2$17βG)) [1–3]. It also transports both the reduced and the oxidized forms of glutathione (GSH) and thus contributes to the many physiological and pathological processes influenced by these small peptides, including oxidative stress [2,4].

The functional core structure of MRP1, like most ABC proteins, consists of two membrane spanning domains (MSD1 and MSD2) and two nucleotide binding domains (NBD1 and NBD2) which bind ATP and catalyze its hydrolysis to provide the energy necessary for the transport process [5]. Several ABCC subfamily members, including MRP1, have an additional, third MSD (MSD0) that precedes the four domain core structure (Fig. 1A) [3,6]. The transmembrane (TM) α-helices of MSD1 and MSD2 form the substrate translocation pathway and are brought into proximity to the NBDs through the cytoplasmic (or luminal) loops (CLs) that connect the TMs (Fig. 1B) [7].

Our recent studies have focused on understanding the functional role played by the cytoplasmic loop (CL5) that connects TM9 to TM10 in MSD1 of MRP1. CL5 contains a high density of charged residues, some of which are critically important for both the expression and the

Abbreviations: 4-PBA, 4-phenylbutyric acid; ABC, ATP-binding cassette; CL, cytoplasmic loop; LTC_4, leukotriene C_4; MRP1, multidrug resistance protein 1; MSD, membrane spanning domain; NBD, nucleotide binding domain; PEG, polyethylene glycol; TBS, Tris-buffered saline; TM, transmembrane; TMAO, trimethylamine-*N*-oxide

* Corresponding author at: Division of Cancer Biology & Genetics, Queen's University Cancer Research Institute, Kingston, ON K7L 3N6, Canada. Tel.: +1 613 533 2636; fax: +1 613 533 6830.
E-mail address: spc.cole@queensu.ca (S.P.C. Cole).
[1] Present address: Department of Cell and Molecular Physiology, Loyola University Chicago, Chicago, IL 60153, USA.

0005-2736/$ – see front matter © 2013 Elsevier B.V. All rights reserved.
http://dx.doi.org/10.1016/j.bbamem.2013.11.002

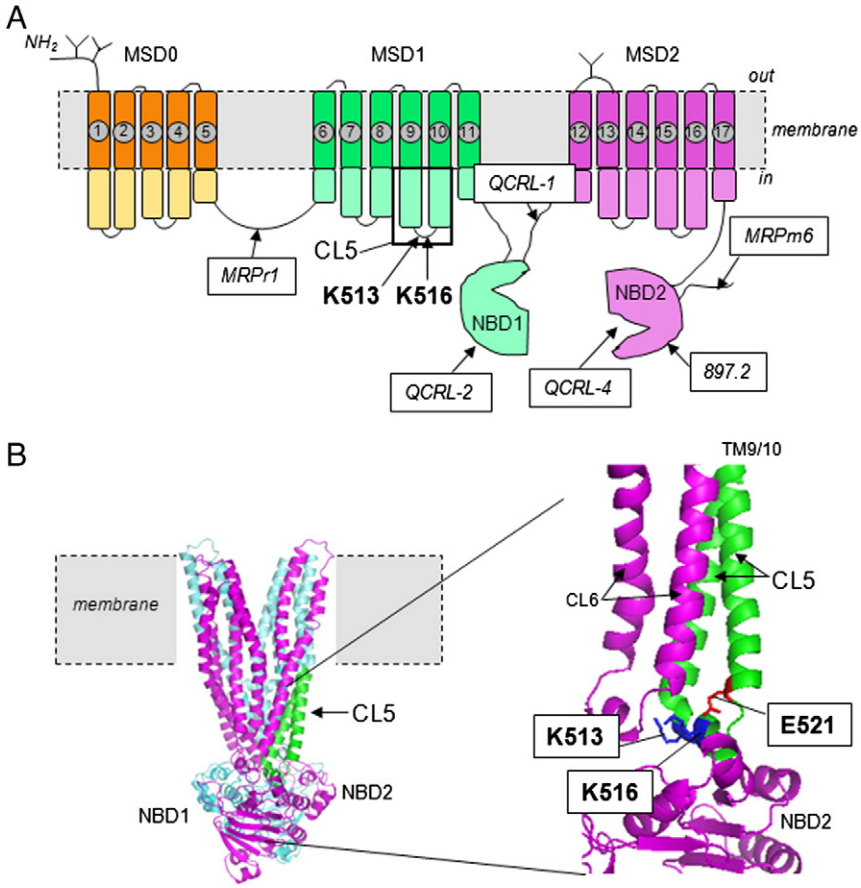

Fig. 1. Secondary structure and homology models of MRP1. (A) Shown is a predicted secondary structure of MRP1 indicating the sites of *N*-glycosylation, the location of K513 and K516 in CL5, and the epitopes detected by the mAbs used in this study. (B) Three-dimensional homology model of MRP1 (lacking MSD0) generated using the crystal structure of nucleotide bound *S. aureus* Sav1866 as template and created using PyMOL [48]; expanded on the right is the region of MRP1 with the predicted location of Lys^{513} and Lys^{516} *(blue)* in the coupling helix of CL5 at the interface with NBD2; and Glu^{521} (*red*) in the α-helix ascending toward the plasma membrane. CL5 (*green*); MSD1 and NBD1 (*cyan*); MSD2 and NBD2 (*magenta*).

function of MRP1. Thus, Ala substitution of Arg^{501}, Glu^{507} or Arg^{532} caused a significant reduction in organic anion transport activity while Ala substitution of Lys^{513}, Lys^{516}, Glu^{521} or Glu^{535} abrogated MRP1 expression by disrupting the folding and assembly of the transporter, targeting it for degradation by the proteasome [8,9].

In the case of three of these misfolded CL5 mutants (K513A, E521A and E535A), plasma membrane MRP1 levels could be improved significantly by exposing transfected HEK cells to the widely used chemical chaperone, 4-phenylbutyric acid (4-PBA) [9,10]. Although the 4-PBA-rescued E521A and E535A mutants were stably expressed, they exhibited mechanistically distinct transport deficiencies that were associated with different structural conformations of the transporter that in turn indicated that the folding and assembly processes for MRP1 are distinct from those of its homolog CFTR [9].

In contrast to E521A and E535A, the 4-PBA rescued K513A mutant exhibited transport properties comparable to wild-type MRP1. Consequently, the failure of 4-PBA to rescue expression of the fourth processing mutant, K516A, was unexpected, particularly since Lys^{516} is within one turn of Lys^{513} in the same α-helix (the so-called coupling α-helix) that atomic homology models predict runs roughly parallel to the plasma membrane and interfaces with NBD1 and NBD2 [7,8]. In the present study, we have further investigated the relative abilities of several chemical chaperones to rescue the expression and/or function of K513A and K516A to better understand the distinct roles that Lys^{513} and Lys^{516} play in promoting the proper folding and assembly of MRP1, and its trafficking to the plasma membrane.

2. Materials and methods

2.1. Materials

[14,15,19,20-^{3}H]LTC_4 (158 Ci mmol^{-1}) and [6,7-^{3}H]$E_2$17βG (45 Ci mmol^{-1}) were purchased from PerkinElmer Life and Analytical Sciences (Woodbridge, ON, Canada). 8-Azido-[α-^{32}P] ATP (3.7 Ci mmol^{-1}) was from Affinity Photoprobes (Lexington, KY). LTC_4 was purchased from Calbiochem (San Diego, CA) and $E_2$17βG, nucleotides, DMSO, PEG (polyethylene glycol 400), trimethylamine-*N*-oxide (TMAO), 4-PBA, proline, apigenin, diphenylcarbamyl chloride-treated trypsin, sodium orthovanadate, and DAPI were purchased from Sigma (Oakville, ON, Canada). The MRP1-specific mAb 897.2 was a kind gift from Dr. X.B. Chang (Mayo Clinic College of Medicine, Scottsdale, AZ) [11]; murine mAb MRPm6, and rat mAb MRPr1 were kind gifts from Drs. R.J. Scheper and G.L. Scheffer (VU University Medical Center, Amsterdam, NL) [12]; and murine mAbs QCRL-1, QCRL-2 and QCRL-4 were generated and characterized in this laboratory [13–15]. Antibodies against calnexin Na^+/K^+-ATPase (rabbit polyclonal) and α-tubulin (murine mAb IgG) were from Santa Cruz Biotechnology and Sigma Aldrich, respectively.

2.2. Preparation of MRP1-enriched membrane vesicles and measurement of MRP1 levels in HEK293T and Sf9 insect cells

The generation of wild-type, K513A and K516A mutant MRP1 pcDNA3.1 expression vectors has been described previously [8,16].

The vectors (20 μg DNA) were transfected into 90–95% confluent SV40-transformed human embryonic kidney cells (HEK293T) using Lipofectamine 2000 (75 μl) (Invitrogen, Carlsbad, CA). Cells were typically collected after 48 h and membrane vesicles prepared and protein levels determined as before [16].

Wild-type and K516A mutant MRP1 were also cloned into pFastBac vectors (Life Technologies Inc.) for expression in Sf9 insect cells. A 4.7-kb XbaI/KpnI MRP1 fragment was subcloned from the pcDNA3.1 vectors into pFastBac and the sequence integrity confirmed. Recombinant bacmids and baculoviruses were generated as described previously [17]. Sf9 cells were grown in Grace's insect cell medium supplemented with tryptose broth (2 g l^{-1}) and 10% fetal bovine serum. Sf9 cells grown as monolayers were infected at 80% confluency with 1.25 ml of wild-type or K516A MRP1 baculoviruses (8×10^7 IFU ml^{-1}) per 150 mm plate. Cells were collected after 72 h and membrane vesicles prepared and protein quantified as before.

2.3. Detection of MRP1 in HEK293T and Sf9 insect cells

Levels of mutant and wild-type MRP1 were determined by immunoblot analysis using mAb QCRL-1 (IgG1; diluted 1:5000–10,000) [14]. To confirm equal loading of protein, blots were stained with amido black and/or probed with antibodies against α-tubulin (diluted 1:20,000) (for whole cell lysates) or Na^+/K^+-ATPase (diluted 1:1000) (for membrane vesicles). Primary antibody binding was visualized by enhanced chemiluminescence detection using appropriate horseradish peroxidase conjugated secondary antibodies. Densitometry of immunoblots was performed using ImageJ software (http://rsb.info.nih.gov/ij/).

Non-denaturing dot blots of HEK293T membrane vesicles were performed using a 96-well manifold to load 0.5, 1.0 and 2 μg of membrane vesicle protein on a membrane in 100 μl Tris-buffered saline (TBS) per well [15,18]. After washing twice with TBS containing 0.05% Tween 20, the dot blot was removed from the manifold, blocked and probed with mAb QCRL-2 (diluted 1:1000) or mAb QCRL-4 (diluted 1:1000) which detect conformation-dependent epitopes of MRP1 contained within NBD1 (amino acids 617–858) and NBD2 (amino acids 1294–1531), respectively [13,15], followed by horseradish peroxidase conjugated secondary antibody and chemiluminescence detection as before. Equal protein loading of the dot blots was confirmed by amido black staining. Relative levels of MRP1 proteins were estimated by densitometry as before.

2.4. MRP1-mediated uptake of ^{3}H-labeled substrates into membrane vesicles

ATP-dependent uptake of ^{3}H-labeled organic anion substrates by the membrane vesicles was measured using a 96-well plate rapid filtration method [8,19]. In brief, 2 μg of membrane vesicle protein was incubated with 50 nM/10 nCi [^{3}H]LTC_4 for 45 s or 1 min at 23 °C or 400 nM/20 nCi [^{3}H]$E_2$17βG for 1 min at 37 °C, with 10 mM $MgCl_2$, 2 mM AMP or 2 mM ATP, in transport buffer (250 mM sucrose, 50 mM Tris–HCl, pH 7.4). Uptake was stopped by rapid dilution, reactions filtered, and then tritium associated with the vesicles was counted. ATP-dependent uptake was calculated by subtracting uptake in the presence of AMP from uptake in the presence of ATP. Transport assays were carried out in duplicate or triplicate, and results expressed as means and corrected to take into account any differences in levels of mutant MRP1 relative to wild-type MRP1. Kinetic parameters for $E_2$17βG uptake by HEK293T membrane vesicles were determined by measuring ATP-dependent uptake at eight different $E_2$17βG concentrations (range 0.25–25 μM), and K_m and V_{max} values calculated by nonlinear regression and Michaelis–Menten analyses using GraphPad Prism™ software [8].

2.5. Photolabeling of MRP1 by [^{3}H]LTC_4

Wild-type and mutant MRP1 membrane proteins were photolabeled with [^{3}H]LTC_4 essentially as described [20,21]. Briefly, membrane vesicles (50 μg) were incubated with [^{3}H]LTC_4 (120 nCi; 200 nM) and 10 mM $MgCl_2$ at room temperature for 30 min and then frozen in liquid nitrogen. Samples were then alternately irradiated at 302 nm for 1 min and snap-frozen ten times, and the radiolabeled proteins resolved by SDS-PAGE. After fixing and treating the gel with Amplify (GE Healthcare, Baie-d'Urfé, QC, Canada), gels were dried and then exposed to film at −70 °C for the times indicated in the figure legends. Relative levels of [^{3}H]LTC_4 labeling were estimated by densitometry as before.

2.6. Photolabeling of MRP1 with 8-azido-[α-^{32}P]ATP

K513A mutant and wild-type MRP1 from transfected HEK cells were photolabeled with 8-azido-[α-^{32}P]ATP essentially as described [22]. Briefly, membrane vesicles were dispersed in transport buffer containing 5 mM $MgCl_2$ and 5 μM 8-azido-[α-^{32}P]ATP. After 5 min incubation on ice, the samples were cross-linked at 302 nm, washed, and then subjected to SDS-PAGE. After drying, the gel was exposed to film for 2–4 h. K513A mutant and wild-type MRP1 membrane proteins were also incubated in transport buffer containing 5 mM $MgCl_2$, 1 mM freshly prepared sodium orthovanadate, and 5 μM 8-azido-[α-^{32}P]ATP for 15 min at 37 °C to measure orthovanadate-induced trapping of 8-azido-[α-^{32}P]ADP by MRP1. The reactions were stopped, membrane proteins washed, and resuspended before cross-linking at 302 nm [22]. Membrane vesicles were then subjected to SDS-PAGE, and after drying, gels were exposed to film for 12–24 h.

2.7. Limited trypsin digestions

HEK or Sf9 insect cell membrane vesicles (2.0 μg per reaction) enriched for K513A or K516A mutant or wild-type MRP1 were digested with trypsin over a range of trypsin:protein ratios for 15 min essentially as described [9,23]. In the case of HEK293T cell membranes, trypsin:protein ratios ranged from 1:5000 to 2.5:1. For insect cell membranes, the ratios ranged from 1:500 to 1:12.5. Full-length and tryptic fragments of MRP1 were detected using mAb MRPr1 (diluted 1:5000), mAb MRPm6 (diluted 1:1000) and mAb 897.2 (diluted 1:5000) as indicated in the figure legends and whose epitopes have been mapped to amino acids 238–247, 1511–1520 and 1318–1388, respectively [11,12] (Fig. 1A).

3. Results

3.1. K513A and K516A mutants differ in their ability to be rescued by chemical chaperones

The relative effectiveness of glycerol, DMSO, PEG and 4-PBA to rescue the processing mutants K513A and K516A was evaluated by comparing MRP1 protein levels in lysates prepared from transfected HEK293T cells treated with or without these chemical chaperones. As shown in Fig. 2A, all treatments enhanced levels of the K513A mutant to a similar degree while the same treatments did not significantly alter wild-type MRP1 levels indicating that the rescue is not a result of transcriptional upregulation. Confocal microscopy confirmed the plasma membrane localization of the rescued K513A mutants indicating their ability to bypass the quality control mechanisms for protein folding in the endoplasmic reticulum of HEK cells and to traffic to the plasma membrane (Supplemental Fig. S1).

In contrast to K513A, and consistent with our earlier observations [9], exposure of K516A transfected cells to glycerol, DMSO, PEG and 4-PBA only slightly increased MRP1 levels (Fig. 2B). The panel of chemical chaperone treatments was then expanded to include the naturally

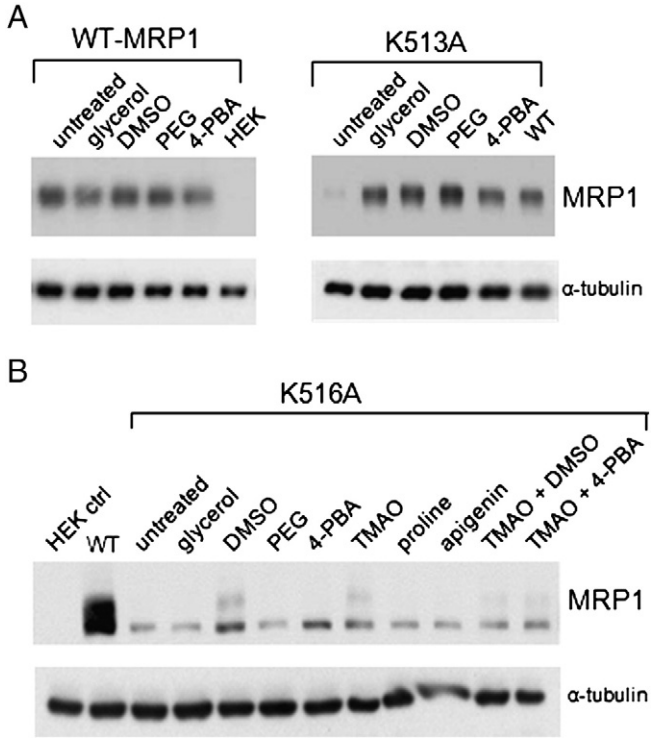

Fig. 2. Effect of chemical chaperones on relative levels of K513A and K516A mutant MRP1 proteins in HEK293T cells. Shown are representative immunoblots of whole cell lysates prepared from HEK293T cells transfected with K513A or K516A mutant or wild-type (WT) MRP1 cDNA expression vectors, with or without exposure to the chemicals indicated at the top of the blots. Untransfected cells were used as a negative control and MRP1 proteins were detected with mAb QCRL-1. Equal protein loading was confirmed by blotting for α-tubulin. (A) WT-MRP1 (*left panel*), K513A (*right panel*); (B) K516A. Similar results were observed for at least two independent transfections.

occurring osmolyte TMAO, proline, and apigenin because these agents have been previously shown to increase levels of processing mutants of other membrane proteins [24–27]. In addition, given the multiple intra- and inter-domain interactions that appear to be involved in the optimal expression of MRP1 at the plasma membrane, it may not be reasonable to expect a single small molecule to 'correct' the conformation and transport activity of K516A. Consequently, the effect of several combinations of chaperones was also explored (Fig. 2B). However, none of the chemicals, alone or in combination, enhanced K516A levels substantially, leading to the conclusion that the folding defects introduced by mutation of Lys^{516} must differ from the defects introduced by mutation of Lys^{513}, despite the close proximity of the two basic residues in the coupling helix in CL5.

3.2. Functional characterization of chemically rescued K513A mutant MRP1 proteins

To determine whether or not the chemically rescued K513A mutants were transport competent, membrane vesicles were prepared (Fig. 3A) and vesicular transport activities were measured using the prototypical organic anion substrates $E_2$17βG and LTC_4. As shown in Fig. 3, [^{3}H]$E_2$17βG and [^{3}H]LTC_4 uptake levels by K513A mutant membrane vesicles prepared from cells treated with 4-PBA or DMSO were comparable to wild-type MRP1. In contrast, vesicles prepared from glycerol or PEG treated cells exhibited transport levels that were just 45–50% those of wild-type MRP1. When $E_2$17βG and LTC_4 uptake levels by wild-type MRP1 membrane vesicles prepared from cells with or without different chemical treatments were determined, no significant differences were observed (data not shown). These results indicate that despite restoring similar levels of the K513A mutant, the chemical chaperones altered MRP1 function to different extents.

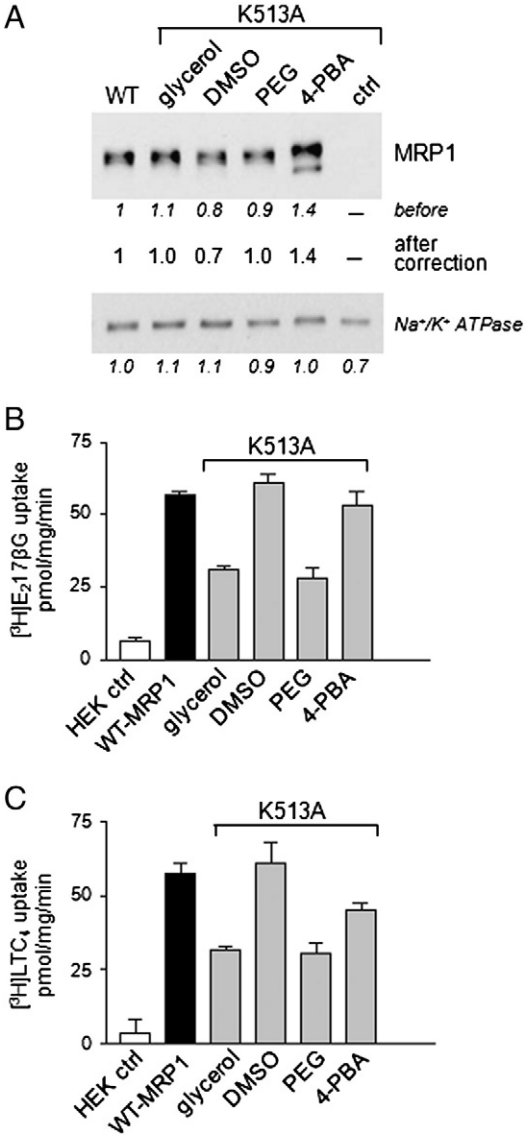

Fig. 3. Effect of chemical chaperones on the levels and vesicular transport activity of K513A mutant MRP1 expressed in HEK cells. (A) Shown is a representative immunoblot of membrane vesicles (1 μg protein per lane) prepared from transfected HEK293T cells, untreated (WT-MRP1) or treated with the indicated chemicals (K513A) for 48 h. Untransfected cells were used as a negative control (*ctrl*). MRP1 was detected with mAb QCRL-1 (*upper panel*), and the relative protein levels estimated by densitometry and corrected as needed for any differences in protein loading as indicated by levels of Na^+/K^+-ATPase (*lower panel*). Similar values were obtained with vesicles prepared from 2–3 additional independent transfections. (B and C), vesicular transport activity of the membrane vesicles shown in (A) was measured as ATP-dependent uptake of (B) [^{3}H]$E_2$17βG and (C) [^{3}H]LTC_4. The results shown are means (±SD) of triplicate determinations in a single experiment. Similar results were obtained in at least one additional experiment with vesicles derived from independent transfections.

3.3. Conformational differences in chemically rescued K513A mutant proteins

To determine whether the transport properties of the K513A mutants rescued by the different chemical chaperones were associated with any differences in protein folding, membrane vesicles containing K513A were subjected to limited trypsinolysis and tryptic fragments detected by immunoblotting with mAbs directed against epitopes in the NH_2-proximal (mAb MRPr1) and COOH-proximal (mAb MRPm6) halves of MRP1 (Fig. 4A) [6,29]. As shown in Fig. 4B (*left panel*), when trypsin digests of wild-type MRP1 were probed with mAb MRPr1, a 115-kDa fragment (N1, corresponding to MSD0–MSD1–NBD1) was first detected followed by a smaller and broader 30- to 45-kDa (N3,

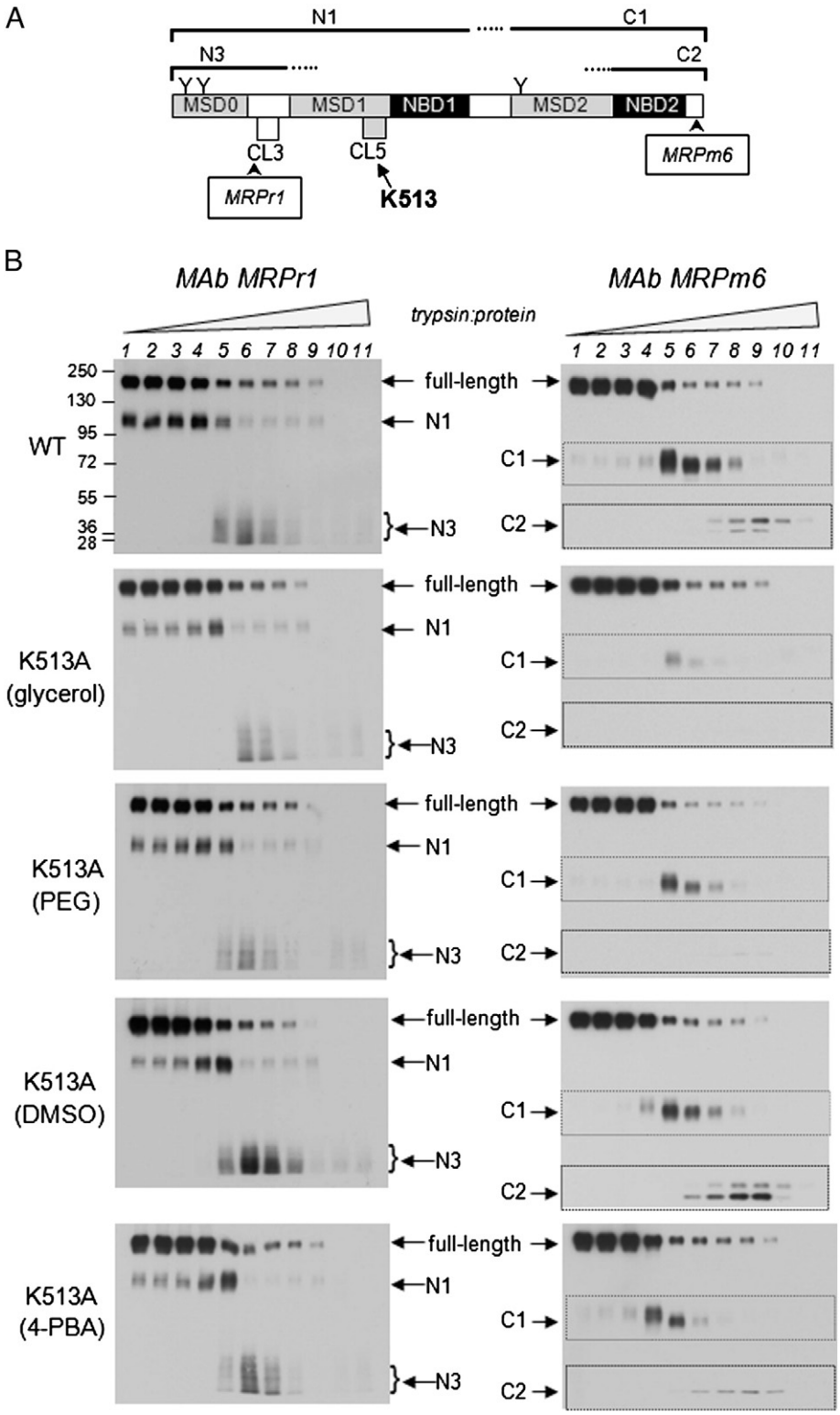

Fig. 4. Limited trypsin digests of chemically rescued K513A mutants and wild-type MRP1 expressed in HEK293T cells. (A) Shown is a schematic representation of glycosylated MRP1 with the sites of initial trypsin cleavage indicated, together with the approximate sizes of the resulting tryptic fragments (N1, N3, C1 and C2), and the epitopes detected by mAbs MRPr1 and MRPm6. (B) Membrane vesicle proteins (2 μg per lane) from cells expressing wild-type MRP1 or K513A mutant MRP1 rescued with the indicated chemical chaperones were incubated at 37 °C for 15 min with trypsin at different trypsin:protein ratios (range 1:5000 to 2.5:1), and then immunoblotted with (*left panel*) mAb MRPr1 and (*right panel*) mAb MRPm6. Trypsin:protein ratios were *(lanes 1–11)*: no trypsin, 1:5000, 1:1000, 1:500, 1:250, 1:100, 1:50, 1:25, 1:10, 1:1, 2.5:1. Similar results were obtained in a second independent experiment.

corresponding to glycosylated MSD0) as the trypsin:protein ratio was increased as expected [6,8,28]. The four chemically rescued K513A mutants had similar tryptic profiles, indicating that the conformation of the NH_2-proximal halves of these mutant proteins were comparable to wild-type MRP1.

To probe for conformational changes in the COOH-proximal halves of the rescued K513A mutants, the trypsin digests were then immunoblotted with mAb MRPm6 (Fig. 4B, *right panel*). Under these conditions, the wild-type MRP1 digests yielded first a larger 75-kDa fragment (C1, corresponding to MSD2–NBD2) which was then cleaved

to generate a smaller 36- to 40-kDa fragment (C2, corresponding to NBD2) as expected [6]. The tryptic profiles for the K513A mutants rescued by DMSO or 4-PBA were similar to wild-type MRP1, suggesting that no significant conformational changes had occurred in the COOH-proximal halves of these mutants. In contrast, the tryptic profiles of the glycerol and PEG rescued K513A mutants were substantially different. Most notably, the NBD2 (C2) fragments were not detectable in the glycerol or PEG rescued K513A proteins. These observations indicate that NBD2 in the glycerol and PEG-rescued K513A mutants is hypersensitive to trypsin suggesting that this region has adopted a more open (less compact) conformation than is the case in wild-type MRP1.

Conformational changes in NBD2 in the glycerol and PEG rescued K513A proteins were further corroborated by taking advantage of two MRP1-specific conformation-dependent antibodies, mAb QCRL-2 (which recognizes a discontinuous epitope within NBD1) and mAb QCRL-4 (which recognizes a discontinuous epitope within NBD2) [15]. Serial dilutions of membrane vesicles prepared under non-denaturing conditions were spotted on a membrane and the dot blots then probed with mAb QCRL-4 (Fig. 5A, *upper panel*), and mAb QCRL-2 (Fig. 5B, *upper panel*); total proteins were detected by staining with amido black (Fig. 5C, *upper panel*); relative signal intensities were quantified by densitometry (Fig. 5, *lower panels*). As shown in Fig. 5A, the immunoreactivity of the glycerol and PEG rescued K513A proteins detected by mAb QCRL-4 was diminished by >50% compared to wild-type MRP1, consistent with substantial changes in the conformation of NBD2. On the other hand, there were no differences in the immunoreactivity of the mutants and wild-type MRP1 detected by mAb QCRL-2 (NBD1) (Fig. 5B). Together with the tryptic fragment analyses (Fig. 4), these results indicate that the transport deficiencies of K513A rescued by glycerol or PEG are associated with a change to a less compact conformation of NBD2 in MRP1.

3.4. $E_2$17βG uptake and [^{3}H]LTC_4 photolabeling of glycerol and PEG rescued K513A MRP1

To further explore the consequences of the conformational changes detected in the glycerol or PEG rescued K513A proteins, kinetic parameters of $E_2$17βG uptake were determined. Consistent with previous studies, wild-type MRP1 transported [^{3}H]$E_2$17βG with a K_m and V_{max} of 4.9 μm and 907 pmol mg^{-1} min^{-1}, respectively [8,19]. The glycerol and PEG rescued K513A proteins exhibited comparable K_m ($E_2$17βG) values of 3.8 and 5.6 μM, respectively, but their V_{max} ($E_2$17βG) values were decreased 3 to 4-fold relative to wild-type MRP1 (230 and 317 pmol mg^{-1} min^{-1}, respectively). [^{3}H]LTC_4 photolabeling of these two rescued K513A proteins and wild-type MRP1 were also comparable (Fig. 6A). Together, these results indicated that the reduced transport levels of the PEG and glycerol rescued K513A mutant were not caused by decreased K_m ($E_2$17βG) or reduced binding of LTC_4 (at 200 nM).

3.5. Photolabeling of glycerol and PEG rescued K513A MRP1 with 8-azido-[α-^{32}P]ATP and orthovanadate-induced trapping of 8-azido-[α-^{32}P]ADP

Since the transport deficiencies of the glycerol- and PEG-rescued K513A proteins were not associated with differences in K_m ($E_2$17βG) or reduced binding of LTC_4 (at 200 nM), the nucleotide interactions of the mutants were examined. First, ATP binding was measured by photolabeling the proteins with 5 μM 8-azido-[α-^{32}P]ATP under conditions of minimal hydrolysis (4 °C). As shown in Fig. 6B, photolabeling of the glycerol- and PEG-rescued K513A proteins at this single concentration of 8-azido-ATP was decreased by 50% and 30%, respectively, compared to wild-type MRP1 (after differences in MRP1 levels were taken into account). Next, the 'catalytic' activity of the rescued mutants was examined by measuring vanadate-induced trapping of azido-[^{32}P]ADP under conditions permissive for ATP hydrolysis [22]. As shown in Fig. 6C, [^{32}P]ADP trapping by glycerol-rescued K513A was 60% lower than trapping by wild-type MRP1 while trapping by the PEG-rescued K513A was 40% lower. Thus, the nucleotide interactions of these mutants have been altered to a degree that correlates well with their reduced transport activities, and are also consistent with the conformational changes in NBD2 detected by limited trypsinolysis, and the MRP1-specific conformation-dependent antibodies.

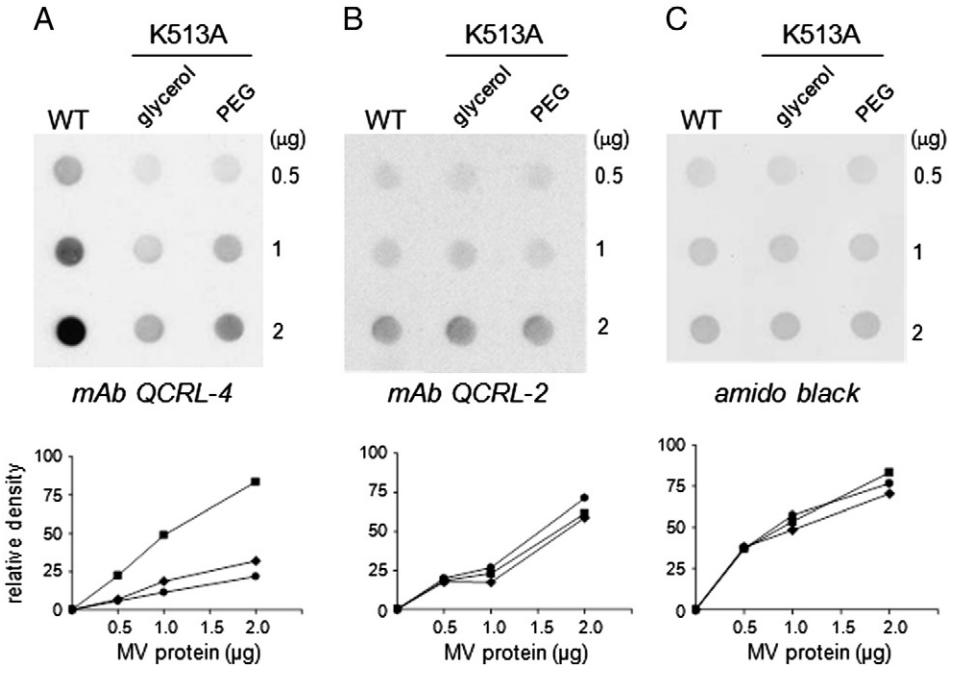

Fig. 5. Immunodot blot analyses of the transport-deficient PEG and glycerol rescued K513A mutant MRP1 with conformation-dependent mAbs against NBD1 and NBD2. Serial dilutions of non-denatured membrane vesicles (corresponding to 0.5, 1 and 2 μg protein) prepared from transfected HEK293T cells expressing K513A mutant (treated with glycerol or PEG for 48 h) or wild-type MRP1 (untreated) were spotted on a membrane as described [18] and then probed with conformation-dependent mAbs (A) QCRL-4 (NBD2); and (B) QCRL-2 (NBD1). (C) Blots were also stained with amido black to confirm protein loading. A graphic representation of the densitometric analyses is shown below each dot blot. WT-MRP1 (■); glycerol-rescued K513A (●); PEG-rescued K513A (◆).

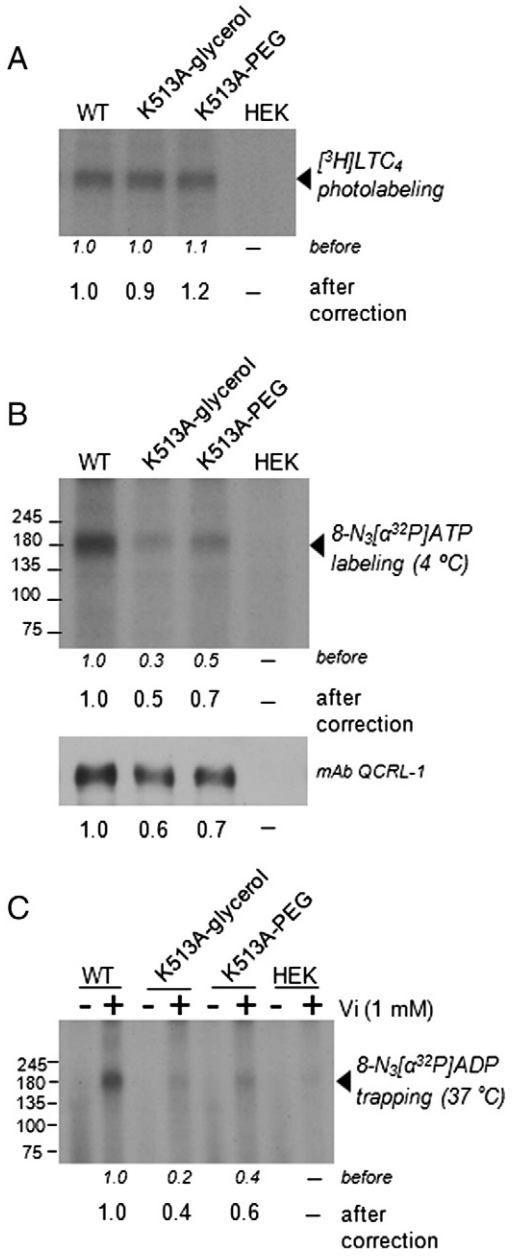

Fig. 6. [^{3}H]LTC$_4$ photolabeling and azido-[α^{32}P]ATP interactions of transport-deficient PEG and glycerol rescued K513A mutant proteins expressed in HEK293T cells. (A) Membrane vesicles (50 μg protein per lane) prepared from transfected HEK293T cells, untreated or treated with glycerol or PEG for 48 h, were incubated with [^{3}H]LTC$_4$ (200 nM; 120 nCi) at room temperature for 30 min, irradiated at 302 nm, and then resolved by SDS-PAGE and processed for fluorography. Shown is a film exposure of 3 days at −70 °C (*upper panel*). Band intensities were determined by densitometry and relative levels of photolabeling calculated after correction for any differences in MRP1 levels as detected with mAb QCRL-1 (panel B, *lower panel*). (B) Membrane vesicles (20 μg protein) from transfected cells, untreated or treated with glycerol or PEG for 48 h, were incubated with 5 μM 8-azido-[α-^{32}P]ATP on ice for 5 min in transport buffer containing 5 mM $MgCl_2$. Samples were irradiated at 302 nm and after removal of unincorporated nucleotides, resolved by SDS-PAGE. The gel was dried and then exposed to film. Relative band intensities were analyzed by densitometry and are indicated by the numbers below the figures, expressed before and after correcting for any differences in MRP1 protein levels (*lower panel*). (C) Vanadate-induced trapping of azido-ADP was measured by incubating membrane vesicles (20 μg protein) at 37 °C with 8-azido-[α-^{32}P]ATP in the presence (+) or absence (−) of freshly prepared sodium orthovanadate for 15 min in transport buffer. Samples were irradiated and processed as before. Similar results were obtained in at least one additional independent experiment.

3.6. Expression and functional characterization of K516A in Sf9 insect cells

Since treatment of HEK293T cells expressing MRP1 K516A with chemical chaperones alone, and in combination, failed to significantly increase levels of this mutant protein (Fig. 2C), K516A was cloned into a baculovirus expression vector and expressed in Sf9 insect cells which exert less stringent quality control mechanisms during biosynthesis of human proteins. As shown in Fig. 7A, this approach was successful since K516A was expressed at levels comparable to those of wild-type MRP1 in insect cells. However, the LTC$_4$ transport activity of the heterologously expressed K516A was reduced by 80% relative to wild-type MRP1 (Fig. 7B). [^{3}H]LTC$_4$ labeling of the heterologously expressed K516A mutant was also diminished by 90% (Fig. 7C), indicating the LTC$_4$ substrate binding site of MRP1 had been compromised.

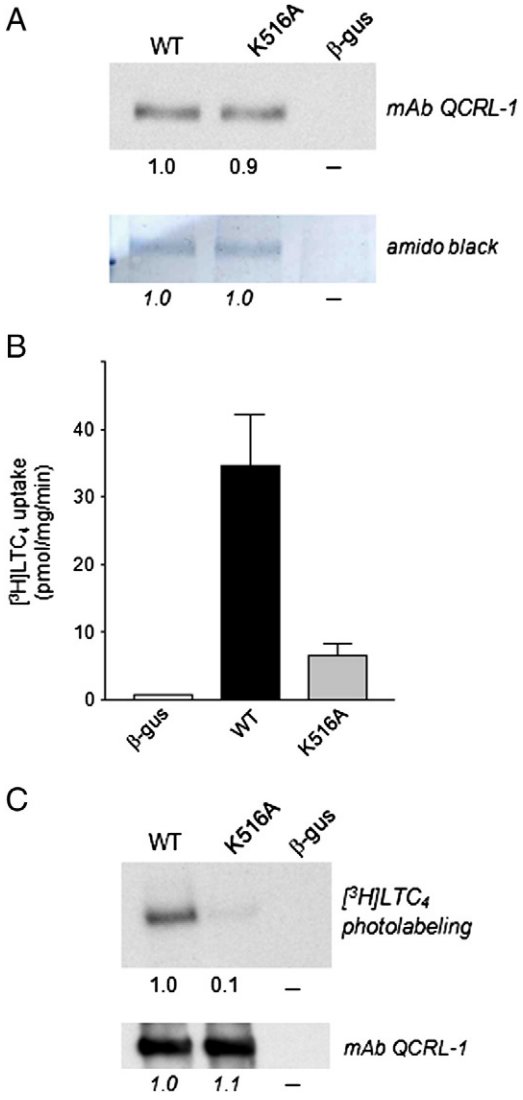

Fig. 7. Expression and function of K516A mutant MRP1 expressed in insect cells. (A) Representative immunoblot of membrane vesicles (1 μg protein per lane) prepared from Sf9 insect cells infected with K516A mutant and wild-type MRP1 recombinant baculoviruses. Membrane vesicles prepared from cells infected with an empty vector were included as a negative control (*β-gus*). MRP1 was detected with mAb QCRL-1 (*upper panel*) and by amido black staining (*lower panel*). (B) [^{3}H]LTC$_4$ transport activity of insect cell membrane vesicles enriched for K516A mutant and wild-type MRP1. ATP-dependent uptake of [^{3}H]LTC$_4$ was measured for 45 s as described in Materials and Methods. The results shown are means (±SD) of three independent experiments. (C) Photolabeling of insect cell membrane vesicles with [^{3}H]LTC$_4$. Control insect cell membrane vesicles (*β-gus*) and vesicles enriched for K516A mutant and wild-type MRP1 (50 μg protein) were photolabeled with [^{3}H]LTC$_4$ as described in the legend to Fig. 6. Shown is a film exposure of 7 days at −70 °C (*upper panel*). Band intensities were determined by densitometry and relative levels of photolabeling calculated taking into account any differences in MRP1 levels as detected by immunoblotting with mAb QCRL-1 (*lower panel*).

3.7. K516A mutation causes 'long range' conformational changes in MSD2

In seeking a structural explanation for the reduced substrate binding of the heterologously expressed K516A mutant, the conformation of the mutant protein was probed by limited trypsinolysis followed by immunoblotting with mAbs directed against epitopes in the NH_2- and COOH-proximal halves of MRP1 as before (Fig. 8A). Differences in the wild-type and K516A tryptic fragmentation patterns were detected with both antibodies. Thus, when probed with mAb MRPr1 (Fig. 8B, *left panel*), fragments of unknown identity (50–65 kDa) accumulated in the case of the K516A mutant but not wild-type MRP1, whereas the trypsin sensitivity of the full-length, as well as the expected N1 and N3 (MSD0) fragments, were quite similar. In contrast, when probed with mAb 897.2 (Fig. 8B, *right panel*) the tryptic fragmentation of the K516A mutant was strikingly different from wild-type MRP1. Thus, the levels of the C1 fragment (MSD2–NBD2) for K516A were substantially reduced relative to wild-type MRP1, despite very similar patterns of disappearance for the two full-length proteins. Furthermore, the levels of C2 fragment (NBD2) were also comparable between the wild-type and K516A mutant suggesting that the trypsin hypersensitivity of the C1 fragment (MSD2–NBD2) of K516A is mainly due to conformational changes in MSD2.

4. Discussion

The folding and assembly of polytopic multidomain membrane proteins, like the ABC transporters, are governed by complex processes that are still far from fully understood. The functional expression of ABC proteins requires not only post- and co-translational intra-domain but also cooperative inter-domain interactions to ensure their stable native conformation(s) are achieved [29–31]. Therefore it is perhaps not surprising that disease-associated misfolding and processing mutations of several ABC proteins have been identified which, despite involving amino acids in different domains, cause retention of the affected protein in the ER and often target it for degradation. In some instances, a mutation in the NBD is involved but other domains, including the cytoplasmic regions of the MSDs that interface with the NBDs, are also known to be important [32–35].

It is commonly presumed that there is a relatively high degree of structural similarity among ABC proteins, and consequently, it would not be unreasonable to assume that the processes governing their folding, assembly and membrane trafficking (and the degradation of misfolded or misassembled mutants) might be also similar. However, there is growing evidence (including our own) that indicates that this is not the case, at least not in all the details [29]. For example, for CFTR, the absence of NBD2 (as in a ΔNBD2-CFTR truncation mutant) does not affect the processing and trafficking of this chloride channel [36], while for MRP1, the integrity of the interface between CL5 and NBD2 interface appears critical for the proper folding and assembly of this transporter [9]. Whether or not this is related to the fact that MRP1 (and some of its homologs) contain 5 rather than the typical 4 domains as found in CFTR (and most other ABC proteins) is not known. It may also be that certain aspects of the co-operative folding and assembly mechanism of each of transporter is unique.

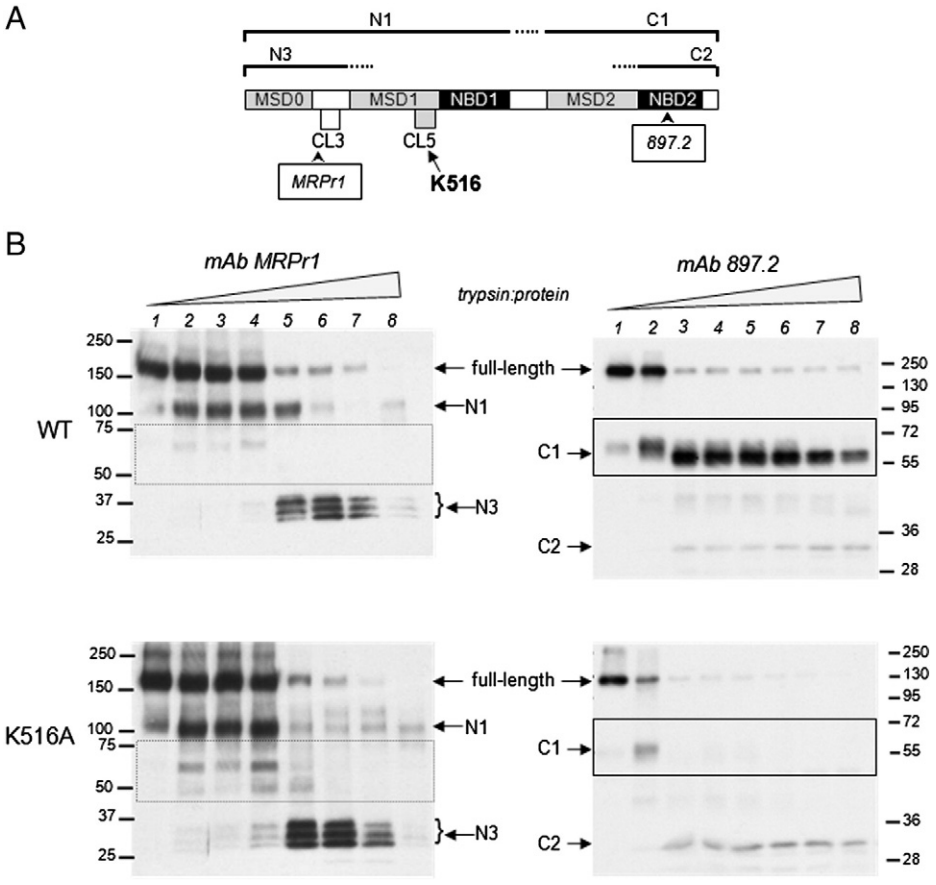

Fig. 8. Limited trypsin digests of transport-deficient K516A mutant MRP1 in insect cell membranes. (A) Shown is a schematic representation of unglycosylated MRP1 with the sites of initial trypsin cleavage indicated, together with the approximate sizes of the resulting tryptic fragments (N1, N3, C1 and C2), and the location of the epitopes detected by mAb MRPr1 and mAb 897.2. (B) Membrane vesicles (2 μg protein) prepared from insect cells expressing transport-deficient K516A mutant and wild-type MRP1 were incubated at 37 °C for 15 min with trypsin at different trypsin:protein ratios (range 1:500 to 1:12.5) and then immunoblotted with (*left panel*) mAb MRPr1 and (*right panel*) mAb 897.2. Trypsin:protein ratios were (*lanes 1–8*): no trypsin, 1:500, 1:230, 1:200, 1:150, 1:100, 1:50, 1:12.5. The boxes highlight significant differences between the patterns of the tryptic fragments of the wild-type and transport-deficient K516A mutant proteins. Similar results were obtained in a second independent experiment.

Low molecular mass chemical chaperones have been used successfully for many years to restore expression and plasma membrane trafficking of misfolded proteins including various mutant ABC proteins [37–39]. Osmolytes like glycerol and PEG are thought to stabilize proteins by increasing protein hydration and reducing the mobility of individual protein domains. In doing so, they prevent aggregation of incompletely folded conformers and promote stabilization by modifying the free energy difference between partially folded proteins and their more compact native structures [24,40]. Hydrophobic compounds such as DMSO and 4-PBA can also promote folding of mutant proteins by reducing the formation of misfolded aggregates and increasing the pool of folding intermediates. However, they can also have an indirect effect by altering the levels of intracellular molecular chaperones [39–42].

In the present study, we have shown that despite the proximity of the affected amino acids to one another in CL5, the MRP1 processing mutants K513A and K516A display remarkable differences in their ability to be functionally rescued by four commonly used chemical chaperones. This implies that although both mutations cause loss of functional MRP1 at the plasma membrane, they do so by distinct molecular mechanisms. In the case of K513A, levels of the mutant protein could be improved to wild-type MRP1 levels by treatment of cells with all four chemical chaperones tested (Fig. 2A) [9]. However, only the 4-PBA and DMSO-rescued K513A mutants displayed organic anion transport activity comparable to wild-type MRP1.

The reduced transport activity of the glycerol- and PEG-rescued K513A mutants indicated that the structural defects introduced by the Lys^{513} substitution were only partially restored by these two chemical chaperones. Differences in trypsin fragmentation patterns and immunoreactivity with conformation-dependent antibodies revealed that the NBD2 region of the glycerol and PEG-rescued K513A transport-deficient MRP1 mutants had adopted a more open, trypsin sensitive conformation than the same region of wild-type MRP1 (or the functionally intact DMSO or 4-PBA rescued K513A mutants). The kinetic analyses of $E_2$17βG transport and the nucleotide labeling results further indicated that the transport deficiencies of the DMSO and PEG-rescued MRP1 K513A proteins were caused by changes in the binding and hydrolysis of ATP. Together, these results allow us to conclude that Lys^{513} plays a critical role in the interactions of CL5 (in MSD1) with NBD2 that are essential for the proper folding and function of the latter domain in MRP1. Molecular dynamics simulations of the homodimeric bacterial ABC transporter Sav1866 indicate that it can adopt a structurally asymmetric transition state where one active site is occupied by ATP in an occluded state while the other site is unoccupied or binds ATP weakly [43]. The latter unoccupied site was in a more open conformation and more distant from the cytoplasmic loop region than was the ATP-bound site. These observations support the suggestion that the K513A mutation in CL5 of MSD1 interferes with the closure of the NBD2 core subdomain making it less able to form a compact interface with CL5.

The biochemical properties and mode of action of 4-PBA, glycerol, DMSO, and PEG are known to vary and it is not clear here why all 4 were equally able to improve K513A levels but glycerol and PEG were unable to functionally rescue the mutant. Whatever the exact mechanisms, it seems that differential responses to chemical chaperones can vary according to the misfolded protein in question [24,41]. Thus, in contrast to MRP1–K513A, glycerol effectively restored the function of CFTR–ΔF508 while DMSO did not [37,39]. On the other hand, a processing mutant of vasopressin V2 receptor (V2R-V206D) responsible for congenital nephrogenic diabetes insipidus was rescued by treatment of cells with DMSO or glycerol but not with TMAO, 4-PBA or by cell growth at subphysiological temperatures [42].

In contrast to K513A, the K516A processing mutant was remarkably resistant to rescue by the chemical chaperones tested. It was also resistant to other osmolytes and chemical chaperones including proline, apigenin, as well as TMAO, alone or in combination with DMSO or 4-PBA. Thus, it appears that Ala-substitution of Lys^{516} causes a more severe folding defect than Ala-substitution of Lys^{513}, and the energy barrier posed by the defect in the former mutant cannot be overcome by small molecular mass chaperones, at least in HEK cells. In this regard, it is of interest that the same charge K513R mutant could be expressed at levels similar to wild-type MRP1 in HEK cells, while levels of the analogous K516R mutant were 40% lower [8]. This indicates that whereas basicity is the most important property of the amino acid side chain at position 513, both the charge and the volume of the side chain contribute to the functionality of the amino acid at position 516. The more stringent requirements on position 516 for MRP1 structure (and function) are also consistent with the greater conservation of Lys^{516} relative to Lys^{513} across both eukaryotic and prokaryotic sequences which makes an evolutionary conserved role for Lys^{516} more likely.

Despite the inability of chemical chaperones to rescue K516A expression in HEK cells, heterologous expression in Sf9 insect cells yielded levels of the mutant transporter comparable to wild-type MRP1 which is likely attributable to the lower stringency of the protein quality control processes in these cells [44–47]. However, despite the robust levels of K516A mutant achieved in this system, the transport activity of this mutant was severely diminished. Thus, LTC_4 transport levels were just 10% those of wild-type MRP1, and the K516A mutant could no longer be photolabeled with this substrate. These observations indicated that the substrate binding pocket of MRP1 had been compromised which in turn suggested structural differences between the K516A mutant and wild-type MRP1 proteins, despite the fact that both were expressed equally well. Support for this conclusion was obtained by comparing the tryptic digest patterns of the two proteins which indicate that the CL5 K516A mutation in MSD1 introduces a change in the COOH-proximal half of MRP1 (MSD2–NBD2) to a more open, trypsin-sensitive conformation. Since the tryptic fragments of NBD2 (C2) in both wild-type and K516A were similar, it may be inferred that this conformational change lies predominantly in MSD2. This is in contrast to the K513A mutant where NBD2 folding was mainly affected.

According to ab initio analyses, both K513A and K516A mutations are predicted to introduce significant rigidity into the tertiary structure of the coupling helix in CL5 where these Lys residues are found. Both mutations modify the turn of the helix such that its interface with NBD2 is altered. However, the orientation of the Lys^{516} side chain may be subject to different constraints than Lys^{513} because the former residue normally relies on bonding interactions with Glu^{521} to help affect the turn of the α-helix at Ala^{519} as the helix makes its way back up to insert into the membrane (Fig. 1B; Supplemental Fig. 2). This difference would provide a plausible explanation for why mutation of Lys^{516} might be more disruptive to normal domain–domain interactions than mutation of Lys^{513}, which in turn, could explain why the K516A mutant is more resistant to rescue by chemical chaperones than K513A.

In conclusion, despite the fact that the affected amino acids of the two processing mutants studied here reside on the same side of the coupling α-helix in CL5, our data indicate that Lys^{513} and Lys^{516} participate in different interdomain interactions during the biosynthesis of MRP1. Together, our results provide new insights into the complex processes required for the proper folding, assembly and membrane expression of MRP1 which may be relevant to other multidomain ABC proteins involved in various genetic and malignant diseases.

Supplementary data to this article can be found online at http://dx.doi.org/10.1016/j.bbamem.2013.11.002.

Acknowledgements

The authors wish to thank Drs. Gwenaëlle Conseil and Alvaro Hernandez for valuable discussions and technical advice, and Meagan Perry for performing the experiments with the insect cells. This work was supported by a grant (MOP-10519) from the Canadian Institutes

for Health Research (S.P.C.C.). S.P.C.C. is Bracken Chair of Genetics and Molecular Medicine and Tier I Canada Research Chair in Cancer Biology.

References

[1] S.P.C. Cole, R.G. Deeley, Transport of glutathione and glutathione conjugates by MRP1, Trends Pharmacol. 27 (2006) 438–446.
[2] S.P.C. Cole, Targeting multidrug resistance protein 1 (MRP1, *ABCC1*): past, present and future, Annu. Rev. Pharmacol. Toxicol. 54 (2014)(http://www.annualreviews.org/doi/abs/10.1146/annurev-pharmtox-011613-135959).
[3] A.J. Slot, S.V. Molinski, S.P.C. Cole, Mammalian multidrug-resistance proteins (MRPs), Essays Biochem. 50 (2011) 179–207.
[4] N. Ballatori, N. Li, F. Fang, J.L. Boyer, W.V. Christian, C.L. Hammond, Glutathione dysregulation and the etiology and progression of human diseases, Front. Biosci. 14 (2009) 2829–2844.
[5] R. Allikmets, M. Dean, Complete characterization of the human ABC gene family, J. Bioenerg. Biomembr. 33 (2001) 475–479.
[6] D.R. Hipfner, K.C. Almquist, E.M. Leslie, J.H. Gerlach, C.E. Grant, R.G. Deeley, S.P.C. Cole, Membrane topology of the multidrug resistance protein (MRP). A study of glycosylation-site mutants reveals an extracytosolic NH_2-terminus, J. Biol. Chem. 272 (1997) 23623–23630.
[7] K. Hollenstein, R.J. Dawson, K.P. Locher, Structure and mechanism of ABC transporter proteins, Curr. Opin. Struct. Biol. 17 (2007) 412–418.
[8] S.H. Iram, S.P.C. Cole, Expression and function of human MRP1 (ABCC1) is dependent on amino acids in cytoplasmic loop 5 and its interface with nucleotide binding domain 2, J. Biol. Chem. 286 (2011) 7202–7213.
[9] S.H. Iram, S.P.C. Cole, Mutation of Glu^{521} or Glu^{535} in cytoplasmic loop 5 causes differential misfolding in multiple domains of multidrug and organic anion transporter MRP1 (ABCC1), J. Biol. Chem. 287 (2012) 7543–7555.
[10] F. Engin, G.S. Hotamisligil, Restoring endoplasmic reticulum function by chemical chaperones: an emerging therapeutic approach for metabolic diseases, Diabetes Obes. Metab. 12 (Suppl. 2) (2010) 108–115.
[11] L. Cui, Y.X. Hou, J.R. Riordan, X.B. Chang, Mutations of the Walker B motif in the first nucleotide binding domain of multidrug resistance protein MRP1 prevent conformational maturation, Arch. Biochem. Biophys. 392 (2001) 153–161.
[12] D.R. Hipfner, M. Gao, G. Scheffer, R.J. Scheper, R.G. Deeley, S.P.C. Cole, Epitope mapping of monoclonal antibodies specific for the 190-kDa multidrug resistance protein (MRP), Br. J. Cancer 78 (1998) 1134–1140.
[13] D.R. Hipfner, S.D. Gauldie, R.G. Deeley, S.P.C. Cole, Detection of the M(r) 190,000 multidrug resistance protein, MRP, with monoclonal antibodies, Cancer Res. 54 (1994) 5788–5792.
[14] D.R. Hipfner, K.C. Almquist, B.D. Stride, R.G. Deeley, S.P.C. Cole, Location of a protease-hypersensitive region in the multidrug resistance protein (MRP) by mapping of the epitope of MRP-specific monoclonal antibody QCRL-1, Cancer Res. 56 (1996) 3307–3314.
[15] D.R. Hipfner, Q. Mao, W. Qiu, E.M. Leslie, M. Gao, R.G. Deeley, S.P.C. Cole, Monoclonal antibodies that inhibit the transport function of the 190-kDa multidrug resistance protein, MRP. Localization of their epitopes to the nucleotide-binding domains of the protein, J. Biol. Chem. 274 (1999) 15420–15426.
[16] K. Ito, S.L. Olsen, W. Qiu, R.G. Deeley, S.P.C. Cole, Mutation of a single conserved tryptophan in multidrug resistance protein 1 (MRP1/ABCC1) results in loss of drug resistance and selective loss of organic anion transport, J. Biol. Chem. 276 (2001) 15616–15624.
[17] M. Gao, H.R. Cui, D.W. Loe, C.E. Grant, K.C. Almquist, S.P.C. Cole, R.G. Deeley, Comparison of the functional characteristics of the nucleotide binding domains of multidrug resistance protein 1, J. Biol. Chem. 275 (2000) 13098–13108.
[18] K. Ito, K.E. Weigl, R.G. Deeley, S.P.C. Cole, Mutation of proline residues in the NH_2-terminal region of the multidrug resistance protein, MRP1 (ABCC1): effects on protein expression, membrane localization, and transport function, Biochim. Biophys. Acta 1615 (2003) 103–114.
[19] I.J. Létourneau, R.G. Deeley, S.P.C. Cole, Functional characterization of non-synonymous single nucleotide polymorphisms in the gene encoding human multidrug resistance protein 1 (MRP1/ABCC1), Pharmacogenet. Genomics 15 (2005) 647–657.
[20] G. Conseil, R.G. Deeley, S.P.C. Cole, Functional importance of three basic residues clustered at the cytosolic interface of transmembrane helix 15 in the multidrug and organic anion transporter MRP1 (ABCC1), J. Biol. Chem. 281 (2006) 43–50.
[21] G. Conseil, A.J. Rothnie, R.G. Deeley, S.P.C. Cole, Multiple roles of charged amino acids in cytoplasmic loop 7 for expression and function of the multidrug and organic anion transporter MRP1 (ABCC1), Mol. Pharmacol. 75 (2009) 397–406.
[22] K. Koike, G. Conseil, E.M. Leslie, R.G. Deeley, S.P.C. Cole, Identification of proline residues in the core cytoplasmic and transmembrane regions of multidrug resistance protein 1 (MRP1/ABCC1) important for transport function, substrate specificity, and nucleotide interactions, J. Biol. Chem. 279 (2004) 12325–12336.
[23] A. Rothnie, R. Callaghan, R.G. Deeley, S.P.C. Cole, Role of GSH in estrone sulfate binding and translocation by the multidrug resistance protein 1 (MRP1, ABCC1), J. Biol. Chem. 281 (2006) 13906–13914.
[24] A. Bandyopadhyay, K. Saxena, N. Kasturia, V. Dalal, N. Bhatt, A. Rajkumar, S. Maity, S. Sengupta, K. Chakraborty, Chemical chaperones assist intracellular folding to buffer mutational variations, Nat. Chem. Biol. 8 (2012) 238–245.
[25] R.S. Rajan, K. Tsumoto, M. Tokunaga, H. Tokunaga, Y. Kito, T. Arakawa, Chemical and pharmacological chaperones: application for recombinant protein production and protein folding diseases, Curr. Med. Chem. 18 (2011) 1–15.
[26] Z. Ignatova, L.M. Gierasch, Inhibition of protein aggregation in vitro and in vivo by a natural osmoprotectant, Proc. Natl. Acad. Sci. U. S. A. 103 (2006) 13357–13361.
[27] M. Lim, K. McKenzie, A.D. Floyd, E. Kwon, P.L. Zeitlin, Modulation of deltaF508 cystic fibrosis transmembrane regulator trafficking and function with 4-phenylbutyrate and flavonoids, Am. J. Respir. Cell Mol. Biol. 31 (2004) 351–357.
[28] Q. Mao, W. Qiu, K.E. Weigl, P.A. Lander, L.B. Tabas, R.L. Shepard, A.H. Dantzig, R.G. Deeley, S.P.C. Cole, GSH-dependent photolabeling of multidrug resistance protein MRP1 (ABCC1) by [^{125}I]LY475776. Evidence of a major binding site in the COOH-proximal membrane spanning domain, J. Biol. Chem. 277 (2002) 28690–28699.
[29] D. Nikles, R. Tampe, Targeted degradation of ABC transporters in health and disease, J. Bioenerg. Biomembr. 39 (2007) 489–497.
[30] S.J. Kim, W.R. Skach, Mechanisms of CFTR folding at the endoplasmic reticulum, Front. Pharmacol. 3 (2012) 1–11(Article 201).
[31] K. Du, G.L. Lukacs, Cooperative assembly and misfolding of CFTR domains in vivo, Mol. Biol. Cell 20 (2009) 1903–1915.
[32] F.S. Seibert, P. Linsdell, T.W. Loo, J.W. Hanrahan, D.M. Clarke, J.R. Riordan, Disease-associated mutations in the fourth cytoplasmic loop of cystic fibrosis transmembrane conductance regulator compromise biosynthetic processing and chloride channel activity, J. Biol. Chem. 271 (1996) 15139–15145.
[33] F.S. Seibert, Y. Jia, C.J. Mathews, J.W. Hanrahan, J.R. Riordan, T.W. Loo, D.M. Clarke, Disease-associated mutations in cytoplasmic loops 1 and 2 of cystic fibrosis transmembrane conductance regulator impede processing or opening of the channel, Biochemistry 36 (1997) 11966–11974.
[34] R. Mor-Cohen, A. Zivelin, N. Rosenberg, M. Shani, S. Muallem, U. Seligsohn, Identification and functional analysis of two novel mutations in multidrug resistance protein 2 gene in Israeli patients with Dubin–Johnson syndrome, J. Biol. Chem. 276 (2001) 36923–36930.
[35] J. Uitto, Q. Li, Q. Jiang, *Pseudoxanthoma elasticum*: molecular genetics and putative pathomechanisms, J. Invest. Dermatol. 130 (2010) 661–670.
[36] Y. Wang, T.W. Loo, M.C. Bartlett, D.M. Clarke, Modulating the folding of P-glycoprotein and cystic fibrosis transmembrane conductance regulator truncation mutants with pharmacological chaperones, Mol. Pharmacol. 71 (2007) 751–758.
[37] S. Sato, C.L. Ward, M.E. Krouse, J.J. Wine, R.R. Kopito, Glycerol reverses the misfolding phenotype of the most common cystic fibrosis mutation, J. Biol. Chem. 271 (1996) 635–638.
[38] D.E. Grove, M.F. Rosser, R.L. Watkins, D.M. Cyr, Mechanisms for rescue of correctable folding defects in CFTR-delta508, Mol. Biol. Cell 20 (2009) 4059–4069.
[39] D.N. Sheppard, Cystic fibrosis: CFTR correctors to the rescue, Chem. Biol. 18 (2011) 145–147.
[40] E. Papp, P. Csermely, Chemical chaperones: mechanisms of action and potential use, Handb. Exp. Pharmacol. 172 (2006) 405–416.
[41] T. Arakawa, D. Ejima, Y. Kita, K. Tsumoto, Small molecule pharmacological chaperones: from thermodynamic stabilization to pharmaceutical drugs, Biochim. Biophys. Acta 1764 (2006) 1677–1687.
[42] J.H. Robben, M. Sze, N.V. Knoers, P.M. Deen, Rescue of vasopressin V2 receptor mutants by chemical chaperones: specificity and mechanism, Mol. Biol. Cell 17 (2006) 379–386.
[43] P.M. Jones, A.M. George, Molecular-dynamics simulations of the ATP/Apo state of a multidrug ATP-binding cassette transporter provide a structural and mechanistic basis for the asymmetric occluded state, Biophys. J. 100 (2011) 3025–3034.
[44] V. Matarazzo, C. Ronin, Human olfactory receptors: recombinant expression in the baculovirus/sf9 insect cell system, functional characterization, and odorant identification, Methods Mol. Biol. 1003 (2013) 109–122.
[45] S. Radner, P.H. Celie, K. Fuchs, W. Sieghart, T.K. Sixma, M. Stornaiuolo, Transient transfection coupled to baculovirus infection for rapid protein expression screening in insect cells, J. Struct. Biol. 179 (2012) 46–55.
[46] F. Bernaudat, A. Frelet-Barrand, N. Pochon, S. Dementin, P. Hivin, S. Boutigny, J.B. Rioux, D. Salvi, D. Seigneurin-Berny, P. Richaud, J. Joyard, D. Pignol, M. Sabaty, T. Desnos, E. Pebay-Peyroula, E. Darrouzet, T. Vernet, N. Rolland, Heterologous expression of membrane proteins: choosing the appropriate host, PLoS One 6 (2011) e29191.
[47] O. Polgar, L.S. Ediriwickrema, R.W. Robey, A. Sharma, R.S. Hegde, Y. Li, S.E. Bates, Arginine 383 is a crucial residue in ABCG2 biogenesis, Biochim. Biophys. Acta 1788 (2009) 1434–1443.
[48] M.K. DeGorter, G. Conseil, R.G. Deeley, R.L. Campbell, S.P.C. Cole, Molecular modeling of the human multidrug resistance protein 1 (MRP1/ABCC1), Biochem. Biophys. Res. Commun. 365 (2008) 29–34.